ACS Macro Letters

Letter

pubs.acs.org/macroletters

pH-Dependent Switchable Permeability from Core–Shell Microcapsules

Joshua M. Grolman,[†,‡] Bora Inci,[†,§] and Jeffrey S. Moore*[,†,‡,§]

[†]Beckman Institute for Advanced Science and Technology, [‡]Department of Materials Science and Engineering, and [§]Department of Chemistry, University of Illinois at Urbana–Champaign, 600 South Mathews Avenue, Urbana, Illinois 61801, United States

Supporting Information

ABSTRACT: We recently reported cationic cyclopolymerization of *o*-vinylbenzaldehydes initiated by boron trifluoride to generate acid-sensitive poly(*o*-(α-alkyl)vinylbenzaldehyde). Herein we report preparation of core–shell microcapsules (μCs) using flow-focusing microfluidic techniques with shells composed of poly(*o*-(α-methyl)vinylbenzaldehyde) (PMVB) that release their payload in response to dilute aqueous acid solution. Release profiles of encapsulated fluorescein isothiocyanate-labeled dextran from μCs are controlled by varying the proton concentration and shell-wall thickness. SEM studies indicate that the system's unique reversible release mechanism involves porosity changes in the shell wall due to microcrack formation.

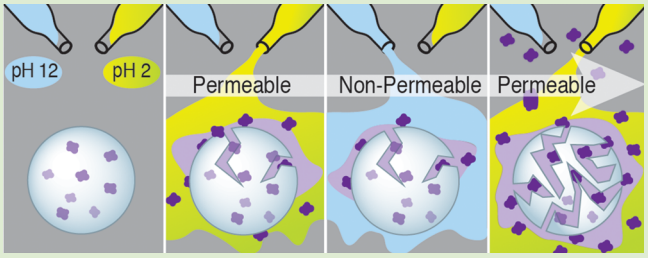

The encapsulation and triggered release of actives are important for applications in drug delivery,[1,2] perfumery,[3] lab-in-a-shell,[4] nutrient preservation,[5] and self-healing materials.[6,7] The ideal delivery vehicles are sufficiently stable to indefinitely store the payload and, following a specific triggering event or upon exposure to particular environments, release the cargo with a controlled profile. One such class of delivery vehicles includes polymeric core–shell microcapsules (μCs), which are mechanically strong, chemically resistant, and compartmentalize volumes of payload. Although many formulations of liquid-filled core–shell μCs have been studied,[7−9] few combine favorable encapsulation properties and controlled payload release[2,10−12] without destruction of the capsules or the use of multicomponent systems. Here we fabricate core–shell μCs in which the shell is composed of acid-degradable poly(*o*-(α-methyl)-vinylbenzaldehyde) (PMVB)[13] with good barrier properties, yet tunable rates of cargo release, by varying the pH and the shell-wall thickness. In comparison with other rapidly degrading polymer capsules,[14] the PMVB system provides acid-catalyzed release characteristics with a change in shell wall porosity while maintaining capsule structural integrity. This unique degradation and pH-tunable release may lend itself to future applications in drug delivery or other fields where multistage and reversible release kinetics from μCs of single polymeric material is desired.

Scheme 1 illustrates the acid-catalyzed mechanism of PMVB degradation. Protonation of the backbone oxygen and subsequent elimination generate indenyl alcohol, 3-methyl-1*H*-inden-1-ol.[13] We imagined this chemistry to be well-suited for the development of μCs with acid-triggered release.

The core–shell μCs were fabricated using a flow-focusing glass capillary device as shown in Figure 1a.[16] PMVB polymer and rhodamine B were dissolved in chloroform to form the oil phase (middle fluid). As described by Phillips and co-workers,

Scheme 1. Proposed Mechanism for the Acid-Catalyzed PMVB Degradation to Yield 3-Methyl-1*H*-inden-1-ol.[15]

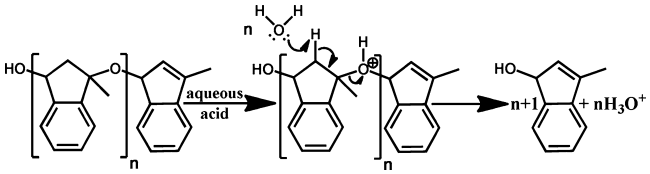

poly(vinyl alcohol) (PVA) was included in the inner (5 wt %) and outer (10 wt %) fluids to balance the osmotic pressure between the interior and exterior of the capsules.[8] Control over capsule morphology and shell-wall thickness was realized by judicious selection of the inner, middle, and outer fluid flow rates. Hexagonally close-packed, monodisperse μCs (Figure 1c) were recovered upon evaporation of chloroform. An inner fluid of 25 mg/mL of FITC-dextran (4 kDa) was used to monitor shell-wall barrier properties and triggered release by acid.

The shell-wall thickness of the μCs was measured by scanning electron microscopy (SEM) (Figure 2). Upon mounting the capsules on SEM stubs, they were ruptured with a razor blade for cross-sectional imaging and coated with approximately 5 nm of gold/palladium. Ten capsules from each sample set were measured for size and shell thickness and averaged together for each flow rate.

In order to confirm the formation of core–shell μCs and provide additional information concerning the shell-wall thickness, fluorescence measurements[17] were performed separately at

Received: March 17, 2015
Accepted: March 31, 2015
Published: April 1, 2015

DOI: 10.1021/acsmacrolett.5b00194
ACS Macro Lett. 2015, 4, 441–445

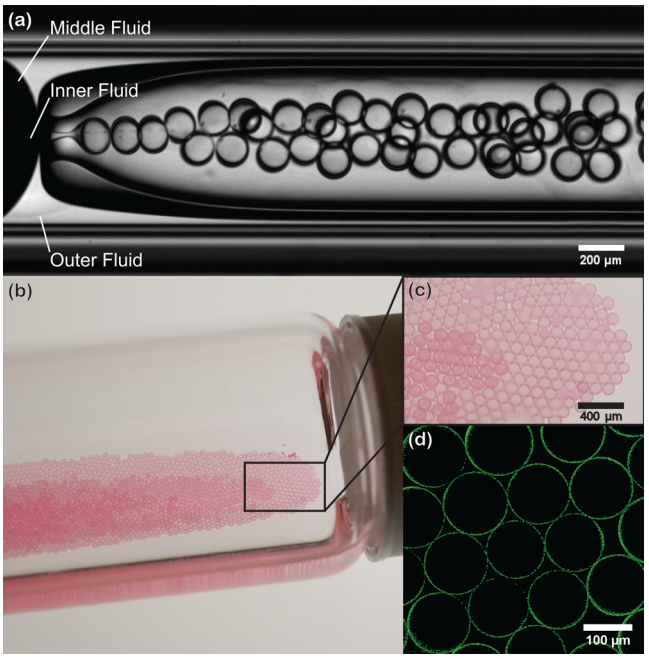

Figure 1. (a) Optical image of a glass capillary flow-focusing device. Inner fluid consisting of 5 wt % PVA and 25 mg/mL of FITC-Dextran (4 dKa), a middle fluid of 10 wt % PMVB with 1 mg/mL of Rhodamine B, and an outer fluid of 10 wt % PVA. (b) Hexagonally packed and dried collected μCs. (c) Magnified view of "b" and (d) confocal fluorescent image of the shell wall of capsules following isolation and drying.

FITC and rhodamine B emission wavelengths to clearly distinguish the capsule inner core and shell wall (Figure 2c–g). The flow-focusing technique readily formed μCs that contain aqueous interiors (FITC-stained) with polymeric shell walls (rhodamine B-stained) and was capable of generating capsules that could be suspended in an aqueous solution of various ionic strengths and buffer compositions.

For SEM and fluorescence characterization, 120 μm sized capsules were selected predominantly for monodispersity and stability. The combination of flow rates (inner–middle–outer: 1000–*X*–8000 in μL/h) generated capsules with a high level of reproducibility so long as *X* remained between 400 and 1000 μL/h. Further variations in flow rates resulted in a loss of stability in monodisperse capsule formation or significant changes in capsule size.

μCs were further characterized for selective dye release by exposing them to various test conditions. Upon addition of freshly prepared aqueous solutions of 12 mM *para*-toluene sulfonic acid (*p*TsOH), 12 mM KOH, 0.1 M NaCl, 0.1 M sodium dodecyl sulfate (SDS), and 0.1 M phosphate buffer, fluorescent images were captured at regular intervals for at least 8 h (Supporting Information (SI) Figure 2). At least 170 capsules were tracked and monitored for each test condition. The percentage of FITC-DEX detected in the capsules was normalized to 25 mg/mL of FITC-DEX emission standards. Sodium chloride solutions and phosphate buffer solutions were tested as controls: the NaCl solution was to determine whether osmotic pressure causes the μCs to release FITC-DEX, and the phosphate buffer solution provided stable pH over the duration of the experiment.

μCs exposed to acids began releasing FITC-DEX immediately, particularly when compared to the control. This release profile was significantly faster, compared to acid-sensitive polymeric

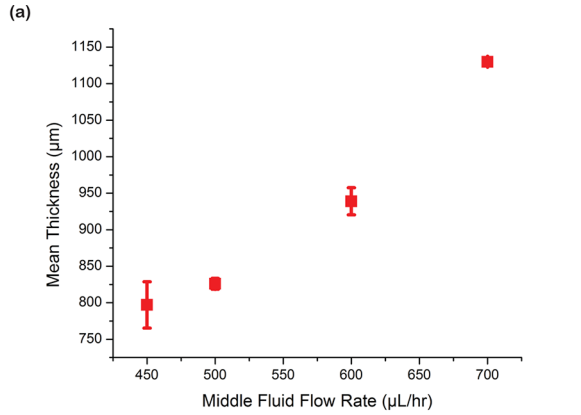

(b)

Flow Rate Inner-Middle-Outer (μL/hr)	Mean Thickness (nm)	Standard Deviation
1000-450-8000	797	±32
1000-500-8000	826	±7.4
1000-600-8000	939	±19
1000-700-8000	1130	±5.6

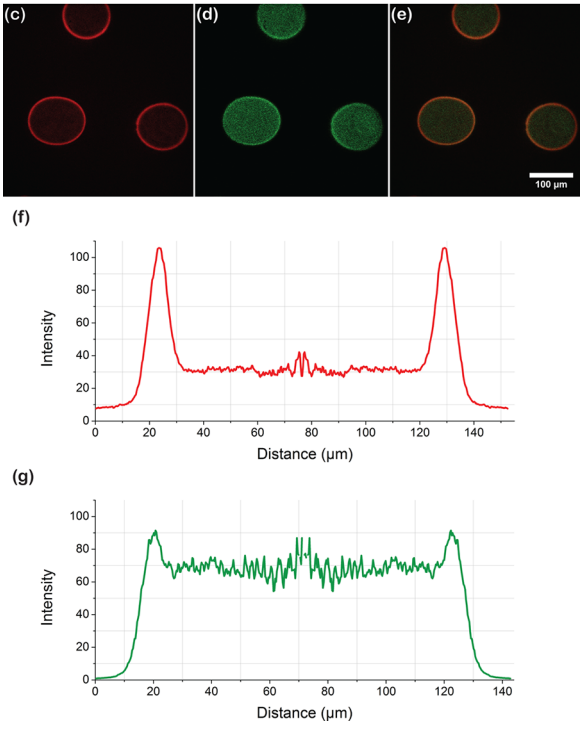

Figure 2. (a,b) Effect of flow rate on the mean shell thickness determined by SEM. For each flow rate, 10 μCs were analyzed, and observed thicknesses were averaged. Fluorescence labeling of capsules with (c) Rhodamine B staining of the middle fluid and polymer shell wall and (d) FITC staining of the inner fluid core. (e) The overlay of image "c" and "d", (f) Rhodamine B, and (g) FITC emission intensity plots of one capsule across the diameter determined by confocal fluorescence microscopy.

μCs of other shell-wall materials reported in the literature that typically take 2 days to release.[8] Sodium chloride triggered very

DOI: 10.1021/acsmacrolett.5b00194
ACS Macro Lett. 2015, 4, 441–445

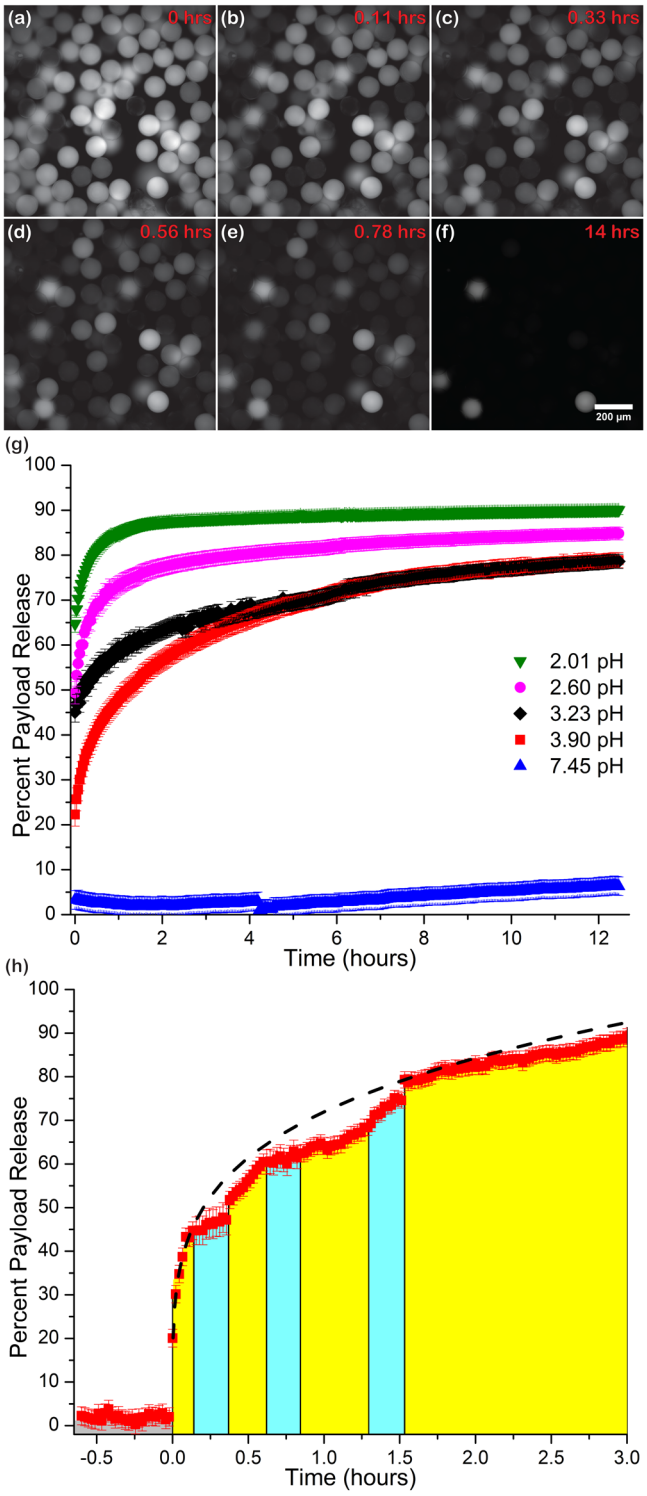

Figure 3. Triggered release of FITC-DEX from acid-triggerable PMVB core−shell μCs when exposed to *p*TsOH solutions in water. (a−f) Optical images of fluorescence emission of the 1130 ± 5.6 nm shell wall for 170 capsules over 14 h. (g) The percentage of 4 kDa FITC-DEX released from 1130 ± 5.6 nm shell capsules in response to single-instance triggering via aqueous *p*TsOH solutions of various concentrations. (h) pH-triggered release from μCs in response to aqueous *p*TsOH (yellow shading) and subsequent quenching with equimolar aqueous KOH (blue shading). The theoretical curve for one single *p*TsOH triggering event is shown as a dotted line.

gradual release, while phosphate buffer showed no significant release. The pH of the supernatants was measured for each of the conditions after the timed fluorescence measurements and was found to be 2.06 for *p*TsOH, 4.92 for NaCl, and 7.47 for phosphate buffer. Increases in shell-wall thickness corresponded to delayed payload release as well as asymptotic tendencies (SI Figures 3 and 9).

The system also demonstrated a strong correlation between acid concentration and the payload release rate. Figure 3g shows the rate of release increased with the hydronium ion concentration. It was observed that pH had an effect on the equilibrium payload release, even though all conditions were from the same batch of μCs with the same shell thickness. To quantify the release character of the capsules, the data were fit to a power law derived from Fickian diffusion (SI Figure 4).[18] As shown below in eq 1, M_t and M_∞ are the cumulative amount of payload released at time t and ∞, respectively. The constant $k_{release}$ relates to the geometry of the microcapsule barrier, while n describes diffusive vs degradative release character. Values of n closer to 1 tend toward degradation-induced, while lower n values indicate Fickian diffusion.[19]

$$\frac{M_t}{M_\infty} = k_{release} t^n \quad (1)$$

Table 1. Curve Fit of Figure 3h to the Power Law Equation

pH	$k_{release}$	n
2.01	49.7	0.194
2.60	58.5	0.117
3.23	73.2	0.0619
3.90	84.5	0.0275

From Table 1, it is evident that there is a strong relationship between hydronium ion concentration and the mechanism by which the payload is released. As shown in the SI Figure 5, the correlation for both $k_{release}$ and n to pH is nonlinear.

Another unique characteristic of this system was the reversible release caused by pH changes that result in "on/off" permeability behavior, as shown in Figure 3h. The μCs were exposed to either neutral or acidic conditions by subsequent equimolar additions of *p*TsOH and KOH, respectively. Upon acid addition, the μCs were in the open state, while neutralizing the pH with the addition of base significantly reduced the payload release rate. Typically, systems require noncovalent shell components to rearrange depending on environmental pH such as lipids[20] or polyelectrolytes.[21] In our case, even though trace PVA still remains despite the washing steps, PVA is fairly pH stable[22] and does not seem to undergo drastic conformational changes within the range we have studied.[23]

ESEM images (Figure 4a−f) were taken to further investigate the mechanism behind the release of FITC-DEX from the polymeric μCs. Images were taken of samples before (Figures 4a,c,e) and after acid exposure to *p*TsOH (Figures 4b,d,f). The capsule images (a−d) were taken after the timed fluorescence measurements, and the thin-film samples (e,f) were gathered before and after exposure to 0.1 M aqueous TFA from one side of a Franz cell over 24 h. The thin films were prepared by drop-casting the polymer dissolved in 1,4-dioxane and allowing the resulting film to air dry.

The ESEM images indicate that exposure to acid tended to cause transverse cracks to propagate through the thickness of the PMVB. This was particularly evident in Figure 4f where the

DOI: 10.1021/acsmacrolett.5b00194
ACS Macro Lett. 2015, 4, 441−445

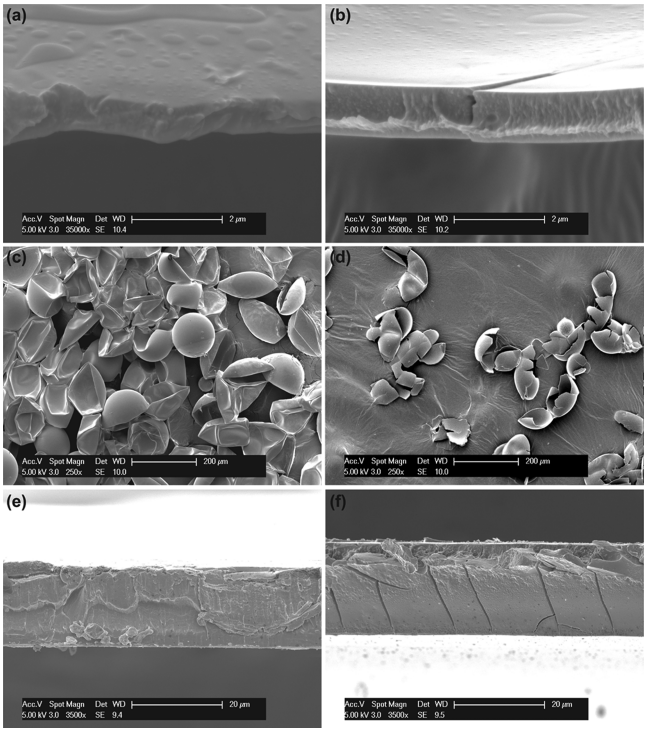

Figure 4. Environmental scanning electron microscopy (ESEM) of capsules and thin films prior to and immediately following acid exposure. (a) Cross-sectional view of a capsule prior to acid exposure. (b) Cross-section of the same sample exposed to 12 mM *p*TsOH and an example of crack formation within the capsules. (c) Macroscopic view of μCs ruptured by razor blade prior to acid exposure. (d) Macroscopic view of a μC ruptured via razor blade after acid exposure. (e) Thin-film cross-section before acid treatment. (f) Thin-film cross-section after 0.1 M aqueous TFA treatment for 24 h.

disjunctions traversed the thin polymer film from the acid-exposed side of the Franz cell to the FITC-DEX-containing side. Curiously, the cracks tended to be approximately 50 nm in gap distance regardless of the thickness of the sample or acid strength. In the Franz cell experimental samples, larger disjunctions formed, but they were predominately seen connected by smaller cracks 50 nm in width. Altogether, these cracks seemed to form a bicontinuous network of 50 nm spacing, which we believe is how the FITC-DEX transferred from the core to the environment.

A most interesting observation is that the polymeric μCs maintain most of their structural stability through routine sample handling procedures; the acid exposure does not significantly compromise the overall capsule integrity. In the absence of razor-blade destruction, both thin films and capsules displayed surfaces covered with longitudinal and latitudinal cracks (SI Figure 6).

A change in mechanical properties can be inferred particularly in Figure 4a and 4b.[24] Figure 4a shows an uneven fracture pattern, characteristic of elastic tearing in polymeric films, while Figure 4b shows the shell-wall fracture characteristic of a brittle material.[25] The data in Figure 4c and 4d also support this, as the original capsules tended to fold over and deform elastically, compared to the relatively brittle nature of acid-exposed μCs.[26] Nanoindentation experiments (SI Figure 7) support this theory of embrittlement, with hardness increasing by more than an order of magnitude after acid exposure and the reduced Young's modulus nearly doubling. The relationship between these mechanical property changes and the chemistry shown in Scheme 1 is presently under investigation.

In conclusion, we have demonstrated that PMVB μCs can be manufactured via microfluidic flow-focusing devices with robust barrier properties in the absence of acidic triggers. Interestingly enough, the degradation mechanisms of this system are unique compared to other stimuli-responsive systems in that it is able to rapidly release active cargo while maintaining core–shell structure. The reversibility of the μC permeability also opens up possibilities for use as a highly sensitive microencapsulation method utilizing acid as a trigger to release payload or capture sample for analysis in response to environmental cues. Mechanistic and size-selective release studies are currently under investigation, and results of these studies will be published in due course.

■ ASSOCIATED CONTENT

Ⓢ Supporting Information

Experimental details, synthetic procedures, and supporting ESEM images, nanoindentor, and payload release graphs. This material is available free of charge via the Internet at http://pubs.acs.org.

■ AUTHOR INFORMATION

Corresponding Author

*E-mail: jsmoore@illinois.edu.

Notes

The authors declare no competing financial interest.

■ ACKNOWLEDGMENTS

We thank Prof. Killian's group for allowing us to use their fluorescence microscope and the Beckman ITG facilities, particularly Dr. Robinson. This work was supported by the Dow Chemical Company through grant RPS 226772 AA. JMG was funded at UIUC from National Science Foundation Grant 0965918 IGERT: Training the Next Generation of Researchers in Cellular and Molecular Mechanics and BioNanotechnology.

■ REFERENCES

(1) Meng, F.; Zhong, Z.; Feijen, J. *Biomacromolecules* **2009**, *10*, 197–209.
(2) Wei, J.; Ju, X.-J.; Zou, X.-Y.; Xie, R.; Wang, W.; Liu, Y.-M.; Chu, L.-Y. *Adv. Funct. Mater.* **2014**, *24*, 3312–3323.
(3) Vaughn, J.; Wu, H.; Efremovska, B.; Olson, D. H.; Mattai, J.; Ortiz, C.; Puchalski, A.; Li, J.; Pan, L. *Chem. Commun.* **2013**, *49*, 5724–5726.
(4) Qiao, Z.-A.; Zhang, P.; Chai, S.-H.; Chi, M.; Veith, G. M.; Gallego, N. C.; Kidder, M.; Dai, S. *J. Am. Chem. Soc.* **2014**, *136*, 11260–11263.
(5) Abraham, S.; Narine, S. S. *J. Nanosci. Nanotechnol.* **2009**, *9*, 6326–6334.
(6) Esser-Kahn, A. P.; Sottos, N. R.; White, S. R.; Moore, J. S. *J. Am. Chem. Soc.* **2010**, *132*, 10266–10268.
(7) Esser-Kahn, A. P.; Odom, S. A.; Sottos, N. R.; White, S. R.; Moore, J. S. *Macromolecules* **2011**, *44*, 5539–5553.
(8) DiLauro, A. M.; Abbaspourrad, A.; Weitz, D. A.; Phillips, S. T. *Macromolecules* **2013**, *46*, 3309–3313.
(9) Peterson, G. I.; Larsen, M. B.; Boydston, A. J. *Macromolecules* **2012**, *45*, 7317–7328.
(10) Tong, W.; Gao, C.; Möhwald, H. *Macromolecules* **2006**, *39*, 335–340.
(11) Skirtach, A. G.; Karageorgiev, P.; Bédard, M. F.; Sukhorukov, G. B.; Möhwald, H. *J. Am. Chem. Soc.* **2008**, *130*, 11572–11573.
(12) Wang, Z.; Möhwald, H.; Gao, C. *Langmuir* **2010**, *27*, 1286–1291.
(13) Inci, B.; Cheng, P.-N.; Beljanski, K.; Moore, J. S. *ACS Macro Lett.* **2013**, *2*, 935–938.

DOI: 10.1021/acsmacrolett.5b00194
ACS Macro Lett. 2015, 4, 441–445

(14) Abbaspourrad, A.; Carroll, N. J.; Kim, S.-H.; Weitz, D. A. *J. Am. Chem. Soc.* **2013**, *135*, 7744−7750.
(15) Ishido, Y.; Aburaki, R.; Kanaoka, S.; Aoshima, S. *Macromolecules* **2010**, *43*, 3141−3144.
(16) Utada, A. S.; Lorenceau, E.; Link, D. R.; Kaplan, P. D.; Stone, H. A.; Weitz, D. A. *Science.* **2005**, *308*, 537−541.
(17) Kim, S.-H.; Kim, J. W.; Cho, J.-C.; Weitz, D. A. *Lab Chip* **2011**, *11*, 3162−3166.
(18) Zhu, A.; Li, F.; Ji, L. *Colloids Surf. B: Biointerfaces* **2012**, *91*, 162−167.
(19) Fu, Y.; Kao, W. J. *Expert Opin. Drug Delivery* **2010**, *7*, 429−444.
(20) Okahata, Y.; Seki, T. *J. Am. Chem. Soc.* **1984**, *106*, 8065−8070.
(21) Lee, D.; Nolte, A. J.; Kunz, A. L.; Rubner, M. F.; Cohen, R. E. *J. Am. Chem. Soc.* **2006**, *128*, 8521−8529.
(22) Byun, H.; Hong, B.; Nam, S. Y.; Jung, S. Y.; Rhim, J. W.; Lee, S. B.; Moon, G. Y. *Macromol. Res.* **2008**, *16*, 189−193.
(23) Hosny, W. M.; Khalaf-Alaa, P. A. *Int. J. Electrochem. Sci.* **2013**, *8*, 1520−1533.
(24) Flory, P. J. *Principles of Polymer Chemistry*; Baker lectures 1948; Cornell University Press: New York, 1953.
(25) Lach, R.; Adhikari, R.; Weidisch, R.; Huy, T. A.; Michler, G. H.; Grellmann, W.; Knoll, K. *J. Mater. Sci.* **2004**, *39*, 1283−1295.
(26) Fu, Y.; Zhang, X. C.; Xuan, F. Z.; Tu, S. T.; Wang, Z. D. *Comput. Mater. Sci.* **2013**, *73*, 113−119.

DOI: 10.1021/acsmacrolett.5b00194
ACS Macro Lett. 2015, 4, 441−445